International Journal of Environment and Geoinformatics 10(2):135-144 (2023)

Research Article

Integrated Method for Classifying Medium Resolution Satellite Remotely Sensed Imagery into Land Use Map

AbdulAzeez Onotu Aliyu[1*], Ebenezer Ayobami Akomolafe[1], Adamu Bala[1], Terwase Toyin Youngu[1], Hassan Musa H[2], Swafiyudeen Bawa[1]

[1] Ahmadu Bello University, Faculty of Environmental Design, Department of Geomatics, Zaria, NIGERIA
[2] Hassan Usman Polytechnic, Department of Quantity Surveying, Katsina, NIGERIA

* Corresponding author: A. O. Aliyu
E-mail: onotuaz@gmail.com

Received 28.07.2022
Accepted 20.05.2023

How to cite: Aliyu, et al., (2023). Integrated Method for Classifying Medium Resolution Satellite Remotely Sensed Imagery into Land Use Map, *International Journal of Environment and Geoinformatics (IJEGEO)*, 10(2): 135-144. doi.10.30897/ijegeo.1150436

Abstract

Several remotely sensed images of various resolutions readily exist. Consequently, different classification algorithms also exist, and are broadly categorized as pixel-based and object-based classification methods. Most times, researchers utilize these coarse resolution images to extract land use and land cover (LULC) of an area. This is usually difficult if distinct land uses are to be derived those is not mutually exclusive and overlap with each other due to proximity and contiguity of the pixels, thus, resulting into "salt and pepper" appearance. In the same vein, object-oriented classification is unsuitable for coarse resolution images. Based on the foregoing, this study provided an integrated method of deriving land use from a coarse satellite image. This was to produce a non-raucous and distinct LULC classes that has the appearance of the object-based image classification technique. Location coordinates of the land uses were acquired with a handheld Global Positioning System (GPS) instrument as primary data. The study classified the image quantitatively (pixel-based) into built-up, water, riparian, cultivated, and uncultivated land cover classes with no mixed pixels, and then qualitatively into educational, commercial, health, residential, and security land use classes that were conflicting due to spectral similarity because they belong to the same built-up pixel group. The total accuracy and kappa coefficient of the pixel-based land cover classification were 92.5 and 94% respectively. The results showed that residential land use occupied an area of 5500.01ha, followed by educational (2800.69ha); security (411.27ha); health (133.88ha); and commercial (109.01ha) respectively. The produced LULC map has a crisp-appearance and distinct classes. The approach would exceedingly overcome the "salt and pepper" effect that has bedevilled the scientific community of remote sensing applications. The output of integrated method can be a vector or raster model depending on the purpose for which it is created.

Keywords: Land use, Land cover, pixel-based classification, integrated method, spectral similarity.

Introduction

LULC maps of an area provide information to help users to understand the current landscape (NRSC, 2015). LULC mapping is important in designing ecosystem services (Abebe et al., 2021). Many studies have been conducted in an attempt to identify an appropriate method for classifying remote sensing data (Xiaoxia et al., 2018; Esetlili et al., 2018). Different algorithms are available for land cover classification, each with its own set of strengths and weaknesses in different environments. Since remote sensing images consist of matrices of pixels, conventional land-cover mapping has been pixel-based (Dean and Smith, 2003). Previously, the majority of LULC classifications were produced via a pixel-based analysis of remotely sensed images. They used either a supervised classification, unsupervised classification or some combination (Enderle and Weih Jr., 2005). In other words, this pixel-based method is also called traditional or conventional method of classifying remotely sensed data.

Land Use and Land Cover (LULC) are related but technically not identical. Land Cover (LC) is whatever that can be observed such as grasses, artificial structure, rocks, bare soil, water (Lambin et al., 2007; Çelik et al., 2019). Land use is the manner in which human beings employ the land and its resources (Ololade et al. 2008; Kaya et al., 2015-2017). In general, land cover is what one can see when one is some distances (e.g. 100m) above the ground and it is also shown by an aerial imagery. Land Use (LU) on the other hand cannot be easily identified from an elevated platform. It requires a researcher's knowledge of the area or identifying it absolutely with a positioning device.

Devhari and Heck, (2009) explained that traditional classification employs multi-spectral classification algorithms, which allocate a pixel to a class based on spectral similarities with the class or other classes. Outcomes of pixel-based methods are frequently raucous and erroneous in nature (Xiaoxia et al., 2018), especially when there are overlapping areas (Chigbu et al., 2015), thereby resulting into mixed pixels (Aliyu, 2015). Aggarwal et al. (2016) pointed out that the spectral information in pixel-based analysis is cogent, but the spatial information is poor, ignoring texture, context, and shape information. Pixel-based analysis is constrained for two reasons: image pixels are not actual geographical objects, and pixel topology is limited.

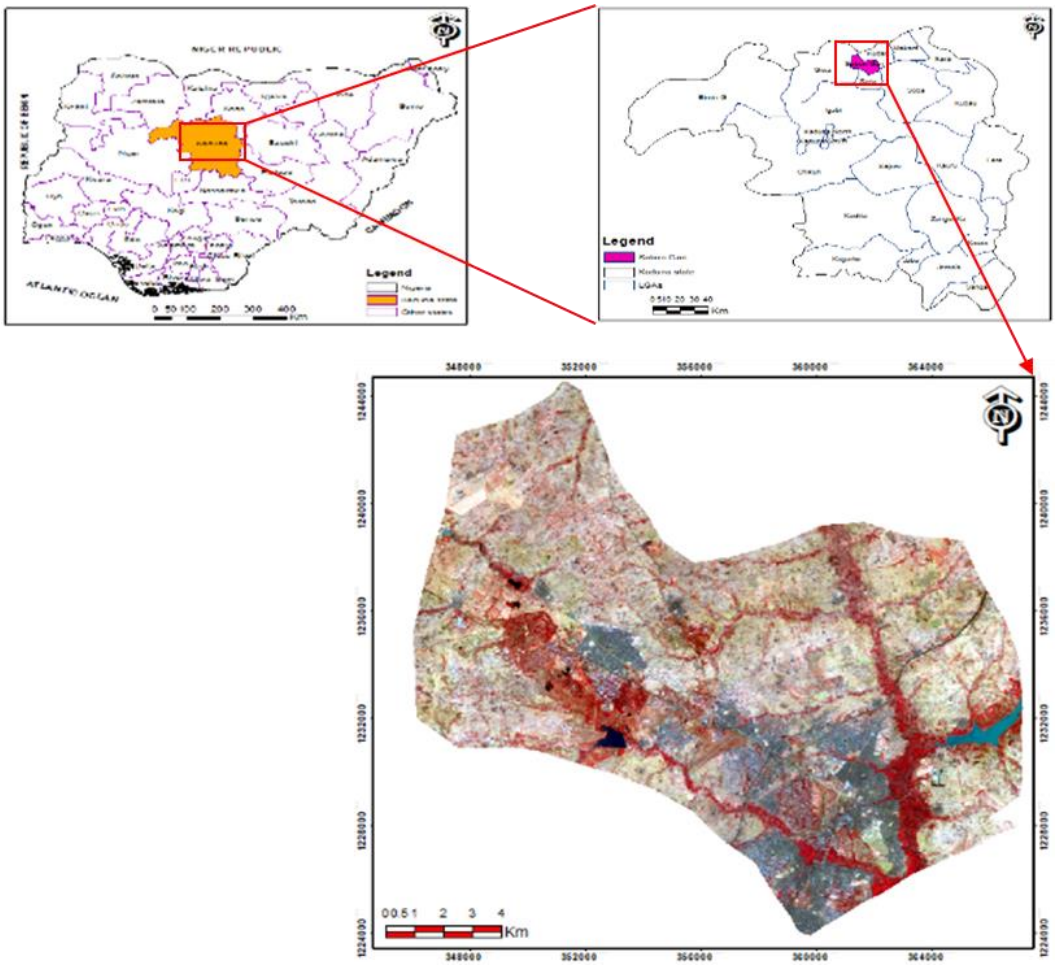

Fig. 1. Inset map of the study area. (a) Map showing Nigeria (b) Map showing Kaduna (c) Map of study area.

Table 1: Characteristic of datasets used and their sources.

S/N	Data type	Data name	Data date	Source	Scale/Resolution	Purpose	Description
1	Primary	GPS locations of land uses	12/2/2020	Fieldwork	Not applicable	For identification of land uses	GPS coordinates of various land uses in easing and northing
2	Secondary	Landsat 8: OLI and TIRS	10/3/2020	http://www.glovis.usgs.gov/	30m spatial resolution except band 8 (panchromatic) with 15m resolution.	Derivation of land use and land cover map.	11 bands multispectral image acquired by OLI and TIRS sensor of Landsat.
3	Secondary	Administrative Map	2020	http://www.gadm.com	Vector file	Study area boundary demarcation.	A map showing political boundaries of Nigeria, its states and LGAs in vector format

Furthermore, with the emergence of Very High Spatial Resolution (VHSR) remote sensing images, pixel-oriented techniques have reached their limits. At VHSR, each pixel represents a region spanning from 0.25 to 2m in size, implying that the complexity and diversity of distinguishable items increases significantly (Qin et al., 2015). Researchers discovered that when pixel-based techniques were applied to high-resolution images, a "salt and pepper" effect was generated, which contributed to the classification's inaccuracy (Weih Jr. and Riggan, 2010).

Object-oriented or auto-object approaches, rather than pixels, provide a viable strategy for classifying high-resolution satellite data (Xiaoxia et al., 2018). In object-oriented approach, the processing units are no longer single pixels but image objects. First, the entire image must be divided into meaningful pixel groups (called segments). Following that, a set of knowledge-based categorization criteria should be defined for each class. The principles cover spectral, spatial, contextual, and textual information. Object-oriented classification is appropriate for very high resolution or radar imagery (Xiaoxia et al., 2018).

Many a time, researches are inevitably confined to low-resolution remote sensing images as a result of difficulty in acquiring a VHSR image, due to the high cost and bureaucracy involved in applying for one. If unique land uses are to be determined from this readily available low-resolution image, they may overlap with other land use and land cover classes owing to proximity, contiguity and lack of the pixels being mutually exclusive. Moreover, image pixels are not actual geographical objects. The derived LULC derivation therefore would results into mixed pixels, thus creating a low-quality classified image having a “salt and pepper” or noisy appearance.

Several studies have carried out LULC classification extensively either as a standalone study or as a method in a study (Bawa et al., 2022; Gondwe et al., 2021; Falaki et al., 2020; Spruce et al., 2020; Kidane et al., 2019; Liping et al., 2018; Mienmany, 2018; Rwanga and Ndambuki, 2017; Hassan et al., 2016; Goodin et al., 2015). However, in the LULC classification, the LU class has frequently been generalized as built-up area, without a proper distinction of its constituents (e.g. commercial, educational, health, recreation, etc.). Interestingly, there exists little or no literatures similar to the current study. It is in the light of this identified problem this study utilized an integrated method of qualitative (vector-based) and quantitative methods (pixel-based classification) to classify Landsat image into land uses and land covers of Sabon Gari area of Kaduna state. This was to produce a non-raucous and distinct LULC classes that has the appearance of the object-based image classification technique.

This aim of the study was achieved through the following objectives: (1) acquire field-collected GPS coordinates to identify different land uses and covers; (2) use supervised classification and visual interpretation to classify the spatial distribution of different LULC; (3) use qualitative techniques to distinctly classify the built-up LU class into various components. This study is descriptive, exploratory, and informative. The motive of the study is to communicate to the scientific community of remote sensing the approach for best classifying a low-resolution remotely sensed image into distinct land uses.

Study area description

The study area is the Sabon Gari local government area of Kaduna state in north-west region of Nigeria. It is located between latitudes 11 15' 18" and 11 04' 07" north of the equator and longitudes 7 35' 24" to 7 47' 01" east of the Greenwich meridian (as shown in Figure 1). It has a land size of 27, 925.86 hectares and an elevation range of 585m to 725m above mean sea level. It had a population of 224,067 in 1991 (NPC, 1991) and 291,358 in 2006 (NPC, 2006), with a projected population of 440,705 in 2020 based on a 3% population growth rate. It includes a variety of land uses, such as residential, educational, commercial, agricultural, health, and security. The rationale for choosing the study area is because it is one of the areas in the state that is highly populous and famous for its economic and educational activities.

Material and Methods

Datasets used

The integrated method was used on a Landsat 8 image OLI and TIRS scene with path/row: 189/52. The primary data are location coordinates of land uses within the study area, which were collected in the field with a Garmin 78S handheld GPS receiver. A high spatial resolution Google image and a Nigeria administrative map (in shapefile format) were also used as ancillary data, as indicated in Table 1. Google Earth software, ENVI v5.2, and ArcGIS v10.5 were used to harmonize, process, and analyze the datasets.

Steps for the classifying technique

The technique used for the classification is divided into steps as shown in Figure 2.

The procedures of the integrated method are as follows:

i. The Landsat image was to be used to derive ten (10) land uses and land covers, namely: residential, educational, commercial, health, security, cultivated, uncultivated, water body, riparian, and rock. Because of the proximity and contiguity of some of the land uses and land covers, such as residential, educational, health, security, and rock classes, there was spectral property similarity (since they are all built-up areas). As a result, it would be very hard to separate this into distinct land uses. They have a surface similarity. As a result, training samples for all built-up areas, cultivated, uncultivated, water body, and riparian classes were initially obtained

from the Landsat image. It was aided by visual analysis, which made use of visual interpretation components such as tone, shape, size, pattern, texture, shadow, and association. Then, the training samples were converted to spectral signature. It is worthy of note that many operations (like filtering, classification etc.) carried out on a single scene remotely sensed imagery does not necessarily require the conversion of digital number (DN) of the image into radiance values. However, for analyses involving comparison of multi-temporal images e.g. Normalized Difference Vegetative Index (NDVI), temperature differences, comparison of multi-sensor data etc., such time-based images should be put into a common radiometric scale. Therefore, the Landsat 8 image utilized in this study was not radiometrically normalized because it was a single scene and did not involve temporal comparison and indices derivation.

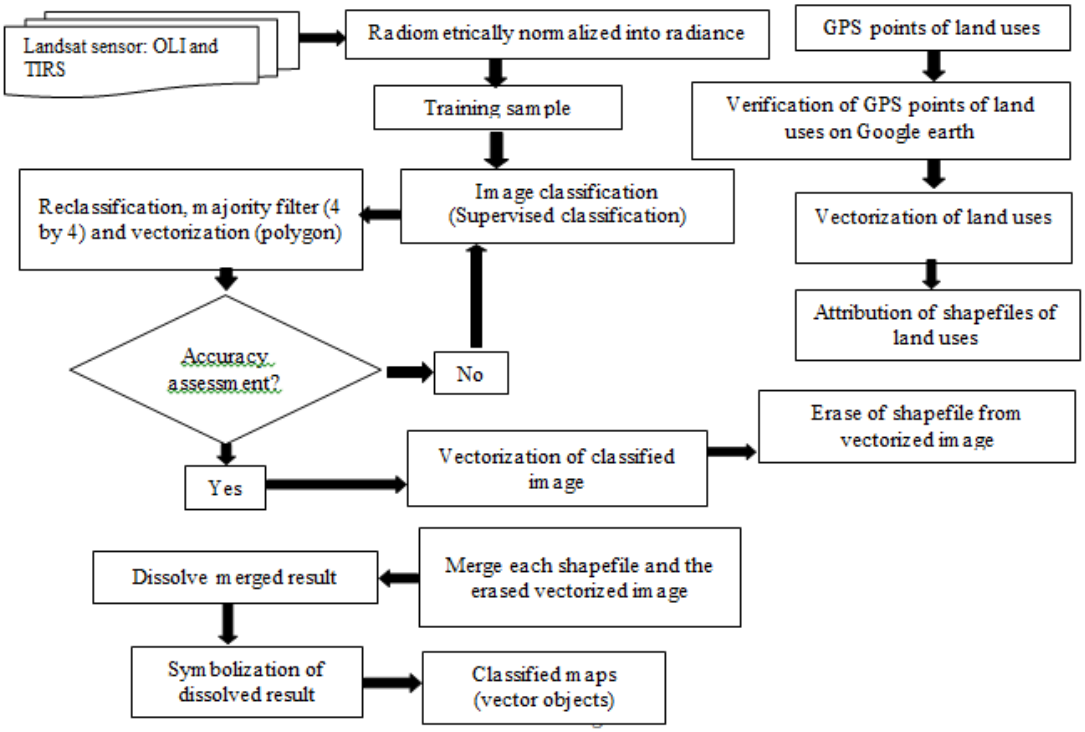

Fig. 2. Workflow diagram for the integrated-classification method

ii. A supervised classification was performed on the Landsat 8 image (USGS, 2018) for the five separate classes in the image (see Table 2) As a parametric decision rule, the maximum likelihood classifier was utilized, which requires that the training data statistics for each class in each band are normally distributed (Ongsomwang, 2007). It also computes the distance between each feature vector and the class means (Gholoobi et al., 2010). The additional classifications were afterwards introduced using a qualitative manner (to be explained in subsequent sections). For classification, ArcGIS v10.5's classification module was employed.

iii. Here, an accuracy assessment of the classified image was carried out to generate a confusion or error matrix. This indicates whether the classification results should be accepted or re-run. As a result, reference pixels were generated using stratified random sampling approach for the classified image. Fifty [50 (i.e. 5 × 10 = 500] reference points were generated. As stated in Anon (2013), the general norm is to gather ten (10) times the number of classes (Aliyu, 2015). Microsoft Excel was used to construct the descriptive assessment of the error matrix (error of omission, commission, etc.) and the discrete multivariate analytical approach (Kappa coefficient).

iv. The classified image was then converted to polygon (vectorized) using "raster to polygon" conversion toolsets in ArcGIS v10.5.

v. For validation, the collected GPS coordinates of land uses, namely: educational, health and security (Table 3), were imported into Google Earth in .kml format. The GPS coordinates of each land use were then polygonized in Google earth, imported as layers, and converted into ArcGIS v10.5 environment using "kml to layer" conversion tool, as shown in Figure 3. Each shapefile of the land use was overlaid on the Landsat 8 image in ArcGIS for validation. For the rock land cover, because of its spectral similarities with the residential class due to their surface resemblance, it was digitized from the image and included in the shapefiles. This operation was possible with the aid of the elements of image interpretation and a thorough knowledge of the study area. Any other built-up area besides education, health, security, and rock was considered a residential area. Because built-up area is a land cover, this meant that the initial classified built-up area was decomposed into other land uses.

Table 2. Description of the LC classes for the Landsat image.

S/N	Training sample	Description	Remarks
1	Built-up	All built-ups areas.	Mixed pixels
2	Uncultivated area	Land consisting of shrubs and other vegetation which is not used for farming activities.	Distinct pixels
3	Water body	Land surface occupied by pond and waterlogged area.	Distinct pixels
4	Riparian	Vegetation situated or taking place along or near the bank of a river.	Distinct pixels
5	Cultivated area	Land occupied or related to agriculture or farming activities.	Distinct pixels

Table 3: Sample of the GPS coordinates of educational LU using Garmin 78S GPS

S/N	Easting (m)	Northing (m)	Height (m)	Code	Remarks
1.	343230	1219744	661	EDU	L.G.E.A. RAFIN YASHI
2.	343622	1232489	685	EDU	LGEA PRY SCH./CLINIC BIJIMI GIWA LGA
3.	344435	1233322	696	EDU	NBC PRIMARY SCHOOL TUDUN BIYE
4.	344547	1220503	674	EDU	L.G.E.A GIDAN ZAKI ZARIA
5.	344632	1218784	649	EDU	L.G.E.A. ANGWAN MALAM SANI PRIMARY SCH.
6.	345411	1222502	692	EDU	L.G.E.A. PRIMARY SCH. KAFIN MARDANNI
7.	346027	1224205	692	EDU	L.G.E.A. PRIMARY SCH
8.	346203	1227284	712	EDU	L.G.E.A. RAFIN YASHI II

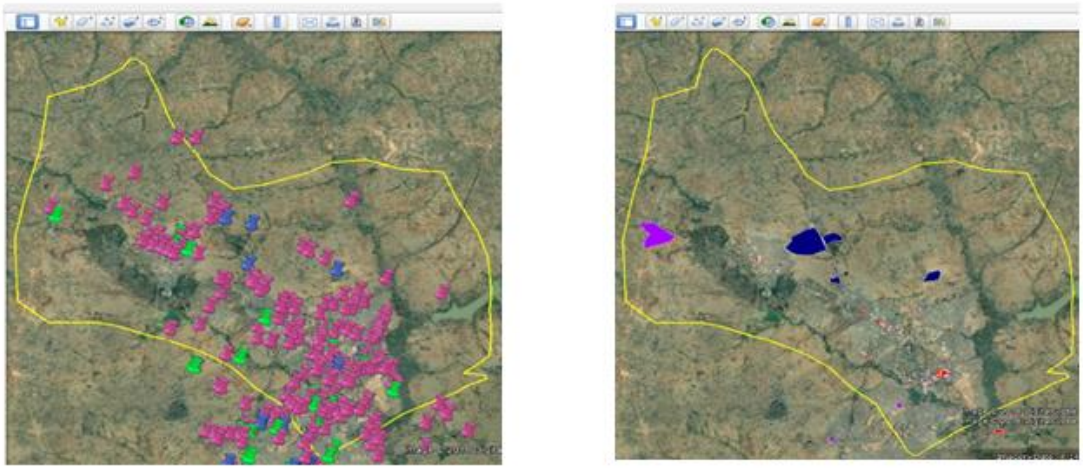

Fig. 3: (a) Screenshot of the GPS locations of educational land use. (b) Digitized polygons of land use in Google earth

Table 4: Description of the identified land use and land cover for the Landsat image.

S/N	Training sample	Type	Description
1	Residential	Land use	Land consisting of buildings for residents
2	Waterbody	Land cover	Land surface consisting of river, lake, stream, pond, etc.
3	Riparian	Land cover	Vegetation situated or taking place along or near the bank of a river.
4	Cultivated	Land cover	Land occupied or related to agriculture or farming activities.
5	Uncultivated	Land cover	Land consisting of shrubs and other vegetation which is not used for farming activities
6	Rock	Land cover	Land surface consisting of rocky and stony materials.
7	Health	Land use	Land consisting of buildings where health activities occur e.g. hospitals, clinics etc.
8	Educational	Land use	Land consisting of buildings for purpose of learning e.g. schools, colleges, polytechnics etc.
9	Commercial	Land use	Land consisting of buildings for purpose of commerce e.g. markets, stores etc
10	Security	Land use	Land consisting of buildings for purpose of security activities e.g. police stations, military barracks etc.

Source: Modified after Anderson (2008) and CORINE (2012)

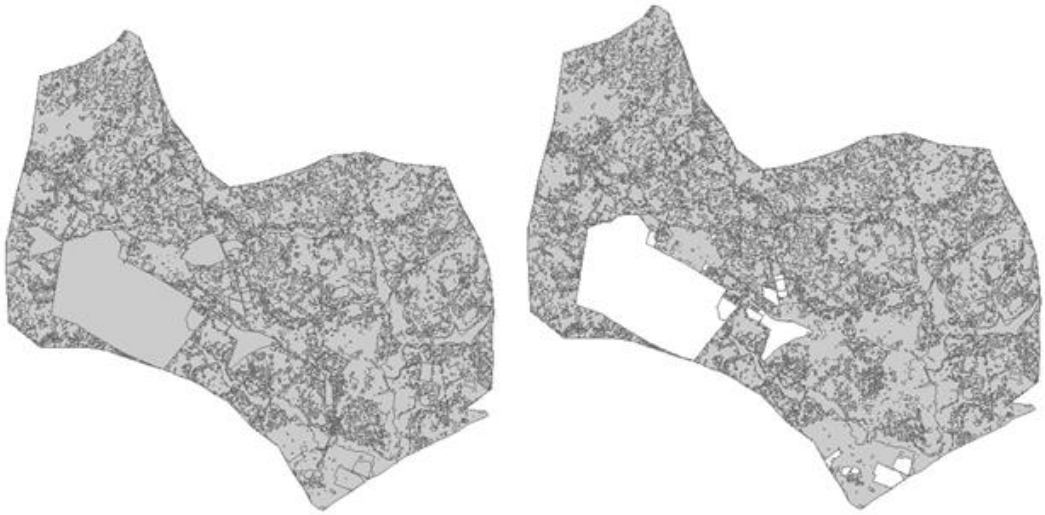

Fig. 4: Integrated method procedure. (a) Merged shapefiles. (b) Dissolved shapefiles

vi. After polygonising (i.e. converting to polygons) all of the land use shapefiles, a new field named "GRIDCODE" was created in the attribute table for each for integration with the supervised classified classes, and an integer number was assigned to each shapefile, namely: rock = 6, health = 7, education = 8, and commercial = 9, and security = 10. This sequence was chosen since the classifications in the previously classified image were in this order: built-up = 1, water body = 2, riparian = 3, cultivated = 4, and uncultivated = 5. In general, this brought the total number of land uses and land covers to ten (10) as indicated in Table 3.
vii. The land use shapefiles were then erased one by one from the "polygonized-classified" picture (the converted classified image to polygon in *step v* above). This was accomplished with the erase tool in ArcMap v10.5.
viii. In *step vii*, each shapefile of the land use and each erased shapefile were combined for the merging operation, and the sequence of merging is indicated in Table 4. Merge tool in ArcMap v10.5 was used. The merged shapefile is shown in Figure 4a.
ix. After that, the merged shapefiles were dissolved to aggregate features based on given attributes. "GRIDCODE attribute field was chosen for dissolving." Dissolve tool in ArcMap v10.5 was used.
x. Figure 4b depicts the dissolved shapefile. Finally, the land use and land cover classes were cartographically represented in ArcMap v10.5 utilizing the "symbology tab" in the layer settings window. The "GRIDCODE" field was then selected in the "categories" list on the "symbology tab" to add all ten (10) classes to the map.

Results and Discussion

Classification accuracy

The most essential challenge in mapping land use and land cover changes using remote sensing are the accuracy of the map. The confusion matrix assessed both the classified image and the reference pixels. Table 4 shows the user and producer accuracies, as well as the associated errors of commission and omission. The overall accuracy and Kappa coefficient were calculated to be 94% and 92.5%, respectively (Table 5). It means that there was 92.5% statistical agreement (Kappa coefficient) between the reference pixels and the supervised categorized map.

Onsomgwong (2007), citing Jensen (2005), who cited Landis and Koch (1977), stated that Kappa coefficient values greater than 80% represent strong agreement or accuracy between the classified map and the reference points; values between 40% and 80% represent moderate agreement; and values less than 40% represent poor agreement or accuracy between the classified map and the reference points.

Land cover map

Figure 5 shows the classified land cover map created using the supervised classification approach. Initially, this land cover map was divided into five (5) categories: built-up, cultivated, uncultivated, waterbody, and riparian. It is a raster data model. All other land uses within the study area, such as residential, commercial, educational, security, and health, are included in the built-up land cover. Land cover refers to land surface characteristics that might be natural, semi-natural, managed, or manufactured. Water, plants, bare earth, and man-made constructions are all part of it. Figure 6 depicts the built-up area, which was then classified into multiple land uses using the integrated method. Waterbody, cultivated, uncultivated, and riparian land cover classes are shown in blue, light green, dark green, and purple (shown in Figure 5).

Land use and land cover map

The classified LULC map using the integrated method is shown in Figure 6. Different colors were used for rendering the LULC classes. The LULC map showed that the residential area (ash color) is concentrated in the southern region of the study area. Riparian vegetation grows along the edge of the waterbody. The educational LU encompassed a huge area and included the

prestigious Ahmadu Bello University (ABU) Zaria, Nigerian College of Aviation Technology (NCAT), Institute of Leather Research, and Nigerian Army School of Military Police, among others. In addition, the commercial area comprises the markets and stores along the roads. Within the study area, there is a lot of uncultivated land.

Table 5: Simple descriptive statistic of the error matrix of the pixel-based classification

S/N	Class	Omission error (%)	Commission error (%)	Producer's accuracy (%)	User's accuracy (%)
1	Water body	0.1	0	90	100
2	Riparian	0	0.09	100	90.91
3	Cultivated	0.04	0.11	96	88.89
4	Uncultivated	0.16	0.02	84	97.67
5	Built-up	0	0.06	100	94.34
	Overall accuracy	94			
	Kappa coefficient	92.5			

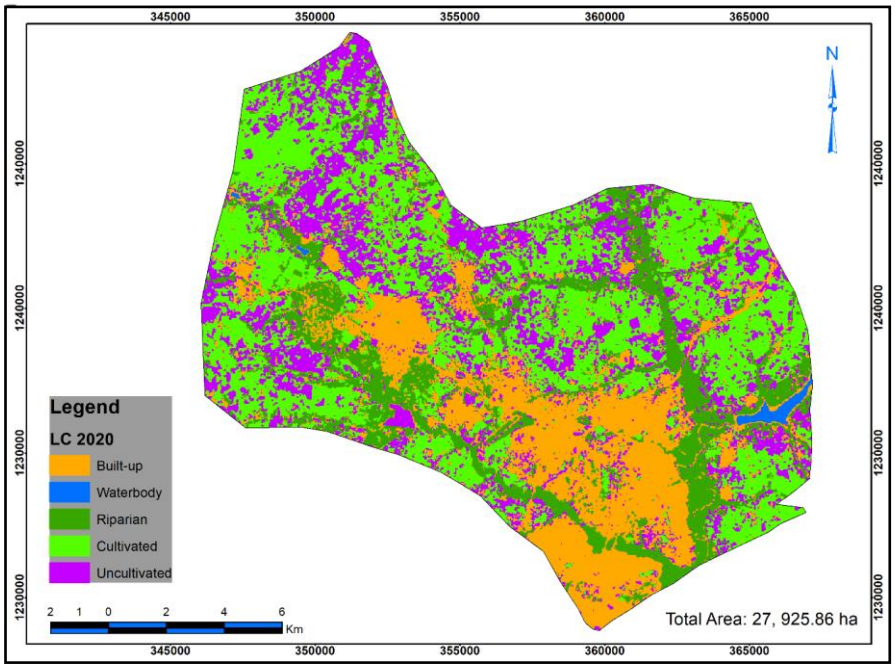

Fig. 5: Classified LC map of the study area of 2020 using supervised classification

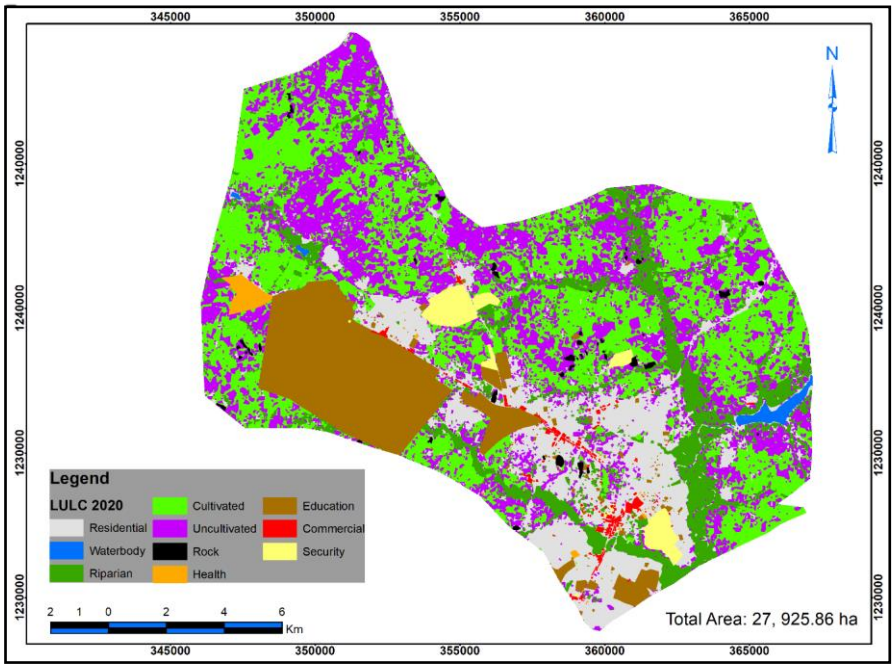

Fig. 6: Classified LULC map of Landsat 2020 using the integrated method

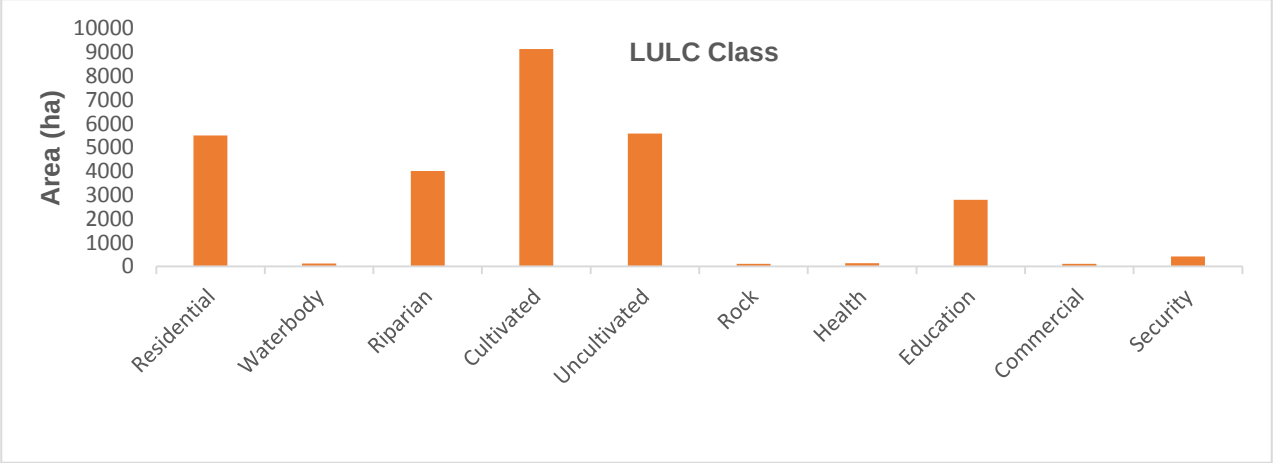

Fig. 7: Land use and land cover area distribution.

The area distribution of the LULC classes is presented in Figure 7. Cultivated area occupied the largest area of 9,139.29ha (i.e. 32.73% of the land) and uncultivated area occupied 5585.91ha (i.e. 20% of the land). Furthermore, residential occupied 5500.01ha, corresponding to 19.7%, implying that there are many people in the study area, whom are attracted by the presence of several higher education institutions. Riparian occupied 4014.19ha (i.e. 14.37% of the total area), indicating agricultural activity near the water body. Educational LU took up 2800.69ha (i.e. 10.03% of the land), which included primary, secondary, and higher institutions. Health, commercial, and security LU classes and took up 133.88ha (0.48%), 109.01ha (0.39%), and 411.27 ha (1.47%) respectively.

Attributes of the integrated method

Comparing the attributes of the pixel-based technique and the integrated method, the classified LULC map produced by the integrated method has the following characteristics: color or spectral, shape, area, outline, and the output was in vector data model (shown in Table 6). It can, however, be rasterized for additional analysis that requires a raster model as an input. Individual classes were distinguished using color/spectral. This feature is shared by both the pixel-based and integrated methods. Furthermore, the shape/form was linked to the grouping or clustering of the same pixels. This attribute is also similar to the segregation feature of the object-based image analysis technique. The area/size attribute corresponded to the polygon nature of each shapefile.

The area/size attributes for the pixel-based technique related correspond to the number of pixel counts multiplied by the area of each pixel. The outline, like the shape/form properties, is responsible for maintaining the spatial contiguity of each shapefile. Furthermore, the traditional pixel-based technique is typically outputted as a raster. Because it is a raster, it has limited geometrical precision and graphics that are inferior to the integrated technique. The attributes of the integrated method enhance the image map, making it clearer and more attractive. As a result, it eliminates the "salt and pepper" appearance that a traditional pixel-based classification would have

Table 6: The attributes of the integrated method

Image classification approach	**Color/spectral**	**Shape/form**	**Area/size**	**Outline**	**Output**
Pixel-based	√	×	√	×	Raster
Integrated method	√	√	√	√	Vector

Conclusion

This study developed an integrated method for classifying coarse resolution optical remotely sensed imagery. The integrated method employs both quantitative (pixel-based) and qualitative (digitization) techniques of classification. It qualitatively digitized the objects of interest utilizing their area, shape, and outline information before classifying them quantitatively. This integrated method mimics the technique (segmentation and classification) of machine-driven object-based image classification. The strategy of the integrated method utilized in this work can overcome the difficulty presented by the pixel-based method, especially when distinguishing unique, contiguous features is required. The integrated technique performs similarly to the object-based image classification method. The study demonstrated the application of the integrated classification method for the classification of ten (10) land use and land cover classes, namely: waterbody, riparian, cultivated, uncultivated, residential, rock, education, commercial, health and security within Sabon-Gari Local Government Area of Kaduna State. The integrated method of classification overcame the problem of classifying of built-up area in a medium remotely sensed imagery into residential, education, health and security land uses. Furthermore, the result was a vector data model (like OBIA does), which is crisper and appealing than using a pixel-based method. The land use and land cover map produced a more realistic representation of the study area.

It is worthy of note that the error matrix for the final LULC map was not computed in this study. This is due to the fact that the LU classes (education, health, commercial, and security) were recorded precisely and "pin-pointly" with a handheld GPS device. Though, as previously noted, an error matrix was created for the pixel-based classification of the first land cover image. The integrated method will assist the Geoinformation Science research community in resolving the "salt and pepper" effect caused by classifying medium remotely sensed images into different land uses. The authors have successfully used this method in the domain of pattern recognition of remotely sensed images for rendering services to stakeholders and governmental agencies. It is worth noting that more research should be conducted to merge the several "disjointed phases" of this integrated technique into a "one-piece" model. This will greatly improve the applicability of the integrated method.

Acknowledgements
The authors would like to acknowledge the U. S. Geological Survey for the provision of the Landsat imagery dataset for this study. The authors also thank the anonymous reviewers for their observations on the study.

Conflict of Interest
There is no conflict of interest among the authors.

References

Abebe, G. Getachew, D., Ewunetu, A. (2021). Analyzing land use/land cover changes and its dynamics using remote sensing and GIS in Gubalafito district, Northeastern Ethiopia. *SN Applied Sciences*, vol. 4 (30) https://doi.org/10.1007/s42452-021-04915-8.

Aggarwal N., Srivastava M., Dutta M. (2016). *Comparative analysis of pixel-based and object-based classification of high-resolution remote sensing images.*

Aliyu A.O. (2015). Mapping, modelling and analysis of desertification in Sokoto state, Nigeria. [Masters Dissertation – Departments of Geomatics, Ahmadu Bello University, Zaria Nigeria], print.

Anderson J. (2008). A comparison of four change detection techniques for two urban areas in the United States.

Anon (2013). Accuracy assessment of an image in ArcMap [Video].

Bawa, S., Akomolafe, E. A., Bala, A., Moses, M., Aliyu, A. O. (2022). Flood susceptibility mapping of urban Zaria, Nigeria. *Asian Conference on Remote Sensing.*

Celik, B., Kaya, Ş., Alganci, U., Seker, DZ. (2019). Assessment of the relationship between land use/cover changes and land surface temperatures: a case study of thermal remote sensing, *FEB Fresenius Environ. Bull.*,3, 541

Chigbu N., Igbokwe J. I., Bello I., Idhoko K., Apeh M. (2015). Comparative study of pixel-based and object-based image analysis in land cover and land use mapping of aba Main Township for environmental sustainability. FIG Working Week, Sofia Bulgaria.

Coordination of Information on the Environment, (CORINE) (2012). CORINE land cover nomenclature conversion to land cover classification system.

Dean A. M., Smith G. M. (2003). An evaluation of per-parcel land covers mapping using maximum likelihood class probabilities. *International Journal of Remote Sensing*. 24: 2905–2920.

Dehvari A., Heck R. J., (2009), Comparison of object-based and pixel-based infrared airborne image classification methods using DEM thematic layer. *Journal of Geography and Regional Planning*, 2 (4). 86-96.

Enderle D., Weih Jr. R. C., (2005). Integrating Supervised and Unsupervised Classification Methods to Develop a more Accurate Land Cover Classification. *Journal of the Arkansas Academy of Science*, 59: 65-73.

Esetlili, M. T., Bektas Balcik, F., Balik Sanli, F., Kalkan, K., Ustuner, M., Goksel, C., Gazioğlu, C., Kurucu, Y. (2018). Comparison of Object and Pixel-Based Classifications For Mapping Crops Using Rapideye Imagery: A Case Study Of Menemen Plain, Turkey. *International Journal of Environment and Geoinformatics*, 5(2), 231-243. https://doi.org/doi.10.30897/ijegeo.442002.

Falaki, M. A., Ahmed, H. T., Akpu, B. (2020). Predictive modeling of desertification in Jibia Local Government Area of Katsina State, Nigeria. *The Egyptian Journal of Remote Sensing and Space Science*, 23(3): 363-370. https://doi.org/10.1016/j.ejrs.2020.04.001.

Gholoobi M., Tayyebi A., Taleyi M., Tayyebi A. H. (2010). Comparing pixel-based and object-based approaches in land use classification in mountainous areas. International Archives of the Photogrammetry, *Remote Sensing and Spatial Information Science*, 38 (8). 789-791.

Global Administrative Areas (GADM). (2018), Nigeria administrative map.

Gondwe, J, F., Lin, S., Munthali, R. M. (2021). Analysis of land use and land cover changes in urban areas using remote sensing: case of Blantyre City. *Discrete Dynamics in Nature and Society (DDNS)*, 22. https://doi.org/10.1155/2021/8011565.

Goodin, D. G., Anibas, K. L., Bezymennyi, M. (2015). Mapping land cover and land use from object-based classification: an example from a complex agricultural landscape. *International Journal of Remote Sensing*, 36 (18): 4702-4723. https://doi.org/10.1080/01431161.2015.1088674.

Hassan, Z., Shabbir, R. Ahmad, S. S., Malik, A. H., Aziz, N., Butt, A., Erum, S. (2016). Dynamics of land use and land cover change (LULCC) using geospatial techniques: a case study of Islamabad Pakistan. *SpringerPlus*, 5, 812. https://doi.org/10.1186/s40064-016-2414-z.

Jensen R. (2005). *Introductory digital image processing: a remote sensing perspective.* 3rd Edition. Practice Hall. P 526.

Kaya, Ş., Çelik, B., Gazioğlu, C., Algancı, U. Şeker, DZ. (2017). Assessment of the Relationship between Land Cover and Land Surface Temperatures Utilizing Remotely Sensed Data: A Case Study of Silivri, *19th MESAEP Symposium on Environmental and Health Inequity*, Rome, ITALY, 3-6 Dec 2017.

Kaya, S., Gazioğlu, C., Sertel, E., Şeker, D.Z., Algancı, U., (2015). Rapid determination of land use/cover changes using data fusion. *The 36th Asian Conference on Remote Sensing "Fostering Resilient Growth in Asia"*, Metro Manila, Filipinler, 19–23 October 2015.

Kidane, M., Bezie, A., Kesete, N., Tolessa, T. (2019). The impact of land use and land cover (LULC) dynamics on soil erosion and sediment yield in Ethiopia. *Heliyon*, vol. 5 (12). https://doi.org/10.1016/j.heliyon.2019.e02981.

Lambin E. F., Geist H. J., Ellis E. (2007). Causes of land-use and land-cover change. in encyclopedia of Earth.

Landis J., Koch G. (1977). *The measurement of observer agreement for categorical data. biometrics.* 33: 159 – 174.

Liping, C., Yujun, S. and Saeed, S. (2018). Monitoring and predicting land use and land cover changes using remote sensing and GIS techniques: A case study of a hilly area, Jiangle, China. *PLoS ONE* 13 (7): e0200493. https://doi.org/10.1371/journal.pone.0200493.

Mienmany, B. (2018). *Analysis of land use and land cover changes and the driving forces: A case study in Kaysone Phomvihan District, Laos*. Master of Science (MSc) dissertation, Faculty of Arts, University of Porto.

National Population Commission (NPC) (1991). National population commission: Nigerian population census reports.

National Population Commission (NPC). (2006). National population commission: Nigerian population census reports.

National Remote Sensing Centre, NRSC (2015). Land Use/Land Cover.

Ololade O., Annegarn H. J., Limpitlaw D., Kneen M. A. (2008). Abstract of Land-Use/Cover Mapping and Change Detection in the Rustenburg Mining Region using Landsat Images, IGARSS.

Ongsomwang S. (2007). Fundamental of remote sensing and digital image processing. School of Remote Sensing, Institute of Science, Suranaree University of Technology.

Qin R., Huang X., Gruen A., Schmitt G., (2015). Object-based 3-d building change detection on multitemporal stereo images. *IEEE Journal of Selected Topics in Applied Earth Observations and Remote Sensing*, 8 (5), 2125-2137.

Rwanga, S. S., Ndambuki, J. M. (2017). Accuracy assessment of land use/land cover classification using remote sensing and GIS. *International Journal of Geosciences*, 8(4): 611-622. https://doi.org/10.4236/ijg.2017.84033.

Spruce, J., Bolten, J., Mohammed, I. N., Srinivasan, R., Lakshmi, V. (2020). Mapping land use land cover change in the Lower Mekong Basin from 1997 to 2010. *Front. Environ. Sci.*, 8 https://doi.org/10.3389/fenvs.2020.00021.

United States Geological Survey (USGS). (2020). Landsat level 1 standard data products. [Image file]

Weih Jr. R. C., Riggan N. D. (2010). Object-based classification vs. pixel-based classification: comparative importance of multi-resolution imagery. International Archives of the Photogrammetry, *Remote Sensing and Spatial Information Science*, 38 (4).

Xiaoxia S., Jixian Z., Zhengjun L. (2018). A comparison of object-oriented and pixel-based classification approachs using Quickbird imagery.